Plant Root Circumnutation-Inspired Penetration in Sand and Clay

Riya Anilkumar[1#] and *Alejandro* Martinez[1]

[1]*University of California Davis, Department of Civil and Environmental Engineering, California, US*
[#]*Corresponding author: ranilkumar@ucdavis.edu*

ABSTRACT

Site investigation (SI) and subsurface exploration are vital for characterizing soil properties. However, a common challenge is the lack of sufficient reaction force to penetrate through stiff crusts or deep layers, leading to refusal. To address this issue, rigs typically have large sizes that can make mobility and accessibility challenging and increase the carbon footprint of SI activities. This paper experimentally investigates a plant root-inspired strategy called circumnutation-inspired motion (CIM) to reduce the vertical penetration forces (F_z) in comparison to quasi-static penetration used for example for Cone Penetration Testing (CPT). The CIM probes have a bent tip end and are rotated at a constant angular velocity (ω) while they are advanced at a constant vertical velocity (v) in uniform specimens of clay and sand. F_z for both soils decay exponentially by factors as high as 10 with increasing relative velocity, defined as the ratio of the tangential to the vertical velocity of the probe tip ($\omega R/v$). Torques for both soils increase with initial increases in $\omega R/v$ which stabilize at higher velocities. While the cumulative total work, calculated for both clay and sand from the measured forces and torques, increases less than 25% for initial increases in $\omega R/v$ between 0 and 0.3π, the F_z can be reduced by around 50%. Thus, CIM penetration can produce significant reductions in F_z in comparison to CPTs while limiting the additional energy consumed. CIM could be implemented to perform site investigation activities, such as obtaining samples or installing sensors, using smaller-sized, light-weight rigs.

Keywords: bio-inspiration, site investigation, efficient penetration

1. Introduction

Site investigation and subsurface exploration is essential for development of civil engineering projects. Commonly used *in-situ* testing methods such as the Cone Penetration Test (CPT) and dilatometer tests (DMT) can face challenges when penetrating stiff crusts (i.e., gravelly or desiccated) or deep layers, leading to early termination of the sounding due to refusal. To provide these large reaction forces, the test rigs often have large sizes, increasing their mobility expenditure as well as their carbon footprint (Purdy et al. 2022; Raymond et al. 2020). The larger size of rigs also creates challenges for performing SI in sites with limited accessibility, such as environmentally protected regions, toes of dams and dense urban areas. Smaller, light-weight equipment for penetrating soil would also be useful in other disciplines such as agriculture, ecology and planetary subsurface exploration (Davidson 1965; Moraes et al. 2014).

Living organisms that interact with soil have evolved to have greater efficiency of burrowing and penetration of soils. Bio-inspiration for geotechnical applications have become increasingly common in the last decade (Martinez et al. 2022). These include the development of burrowing probes and robots (e.g., Huang and Tao 2020; Chen et al. 2021; Dorgan 2015; Chen and Martinez 2023), tree-root inspired anchors and foundations (e.g., Burrall et al. 2020), and snakeskin-inspired surfaces, piles and anchors (e.g., Martinez, Palumbo, and Todd 2019; O'Hara and Martinez 2022)

This study takes inspiration from a strategy used by plant roots, known as circumnutation motion, to penetrate soil using lower vertical reaction forces. During penetration with circumnutation motion, the root tip is slightly bent and rotates as it moves downward into the soil (Migliaccio, Tassone, and Fortunati 2013; Darwin and Darwin 1880; Taylor et al. 2021). The trajectory of the root tip thus traces a helical path (Figure 1a). While this is an irregular helix in most plants, the path of the tip can be idealized as a regular helix as shown in Figure 1b. Thus, a probe that applies motion inspired by root circumnutation can be idealized as cylindrical probe with bend end with a conical tip (Figure 1c). The bent angle of the probe is given by α and the bent length by L_1. The entire probe rotates with an angular velocity of ω and vertically penetrates the soil at a velocity v. The trajectory of the probe tip (blue in Figure 1c) is a helix. The pitch of the helix is determined by the ratio of vertical velocity to angular velocity (v/ω). The slope of the helix is governed by ratio of the tangential to vertical velocity of the probe, referred to as the relative velocity ($\omega R/v$, where R radius form the axis of rotation to the probe tip).

Previous studies on CIM penetration (Chen and Martinez 2023; Anilkumar, Chen, and Martinez 2024) show a dependence of the mobilised vertical penetration force on the relative velocity of the probe. Their results showed that CIM penetration mobilizes lower vertical forces than CPT in sand while a low relative velocity can limit the energy consumption required for penetration.

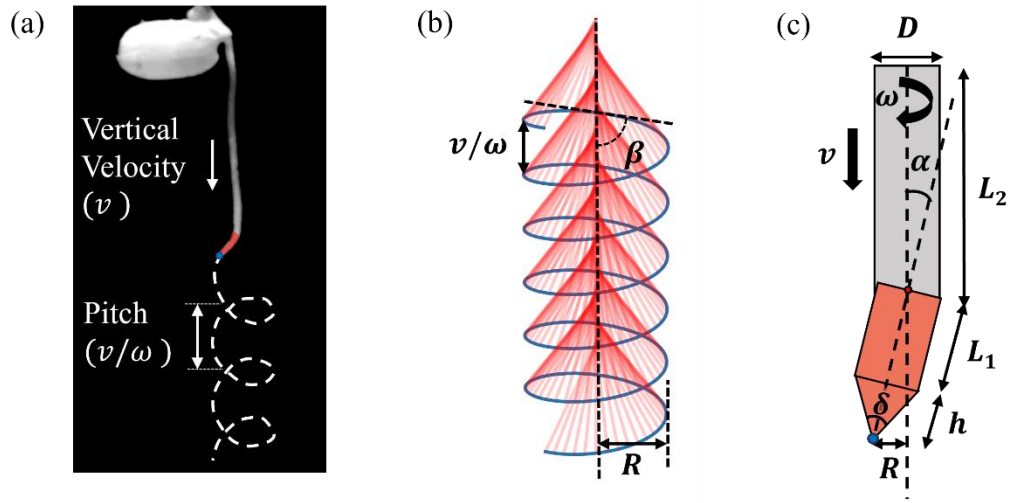

Figure 1. (a) Circumnutation motion in plant roots- bent root end highlighted in red and tip of the root in blue. (b) Idealized helical trajectory of bent end of the root during circumnutation is illustrated (bent end in red and tip in blue). The shape of the helix and helix slope (tan (β)) is determined by the pitch (v/ω) and the radius of the helix (R). (c) Idealized circumnutation inspired motion (CIM) probe design with bent end in red and tip highlighted in blue.

This is in agreement with the results of the experimental investigation by Del Dottore et al. 2017. While these studies explored CIM penetration in sand, limited information is available regarding the effects of soil type.

In this study, CIM penetration in clay is explored with a focus on the effect of changes in relative velocity on the magnitude of mobilized forces and torques and work done to penetrate to a fixed depth. These variations are then compared with corresponding CIM tests obtained in sand as well as with CPT soundings performed in both soil types. The tests in clay also show how CIM can help penetrate through shallow stiff layers that would otherwise lead to early refusal of the soundings.

2. Materials and Methods

2.1. Test setup

A CIM probe of fixed geometry is used to perform experiments in clay and sand deposits. While root diameters may vary, the bent length of the root tips varied from around 2-7 times the root diameter and the bent angle varied from 2° to 45°. For the CIM probes in this study, a diameter (D) of 12.7 mm, an L_1 equal to $1D$ (i.e., 12.7 mm) and an α = 10° is used. The probe is fabricated from aluminum tubing and its conical tip has an apex angle of 60° (Figure 2a). All tests were performed with a spacing of 10 to $12D$ between testing locations or between testing location and the container wall to prevent influence disturbance and boundary effects. Relative velocities ($\omega R/v$) between 0 and 2 π were used as they are representative for the range observed in different plant species (Chen and Martinez 2023). The required relative velocity for each test was obtained by varying ω while keeping v constant for vertical penetration (0.5 mm/s for sand and 5 mm/s for clay, as described below). A CPT probe with the same diameter and apex angle as the CIM probe was used to penetrate soils at the same vertical velocity as the CIM tests for comparison.

The test setup consists of a UR16e robotic arm (Universal Robots) to control v, a stepper motor and gearbox to control ω, the CIM probe and the uniform soil model (Figure 2b). The robot has a vertical force limit of 150 N. The tests were performed by attaching the probe to the motor and gearbox which in turn is attached to the robotic arm. A 6 axis loadcell present at the end of the robotic arm was used to measure the vertical force (F_z) and the relevant torque (T_z) mobilized as the CIM probe penetrates soil. Figure 2 shows the CIM probe and test set up.

2.2. Clay Deposit

All the tests in clay were performed in a single deposit. The clay specimen consisted of kaolin clay consolidated to produce a stiff layer with a highly overconsolidated crust. The specimen was prepared by first consolidating the specimen in 6 sub-layers to specific target stresses and then subjecting the entire deposit to an acceleration of $70g$ in one of the geotechnical centrifuges at the Center for Geotechnical Modeling (CGM) at the University of California Davis. The model was then unloaded from the centrifuge. The use of the press allowed creating a highly overconsolidated crust with a thickness of about 4 cm and OCR values exceeding 70, while the gravitational acceleration of $70g$ applied in the centrifuge led to an average OCR of 70 below the shallow crust. The kaolin clay has a liquid limit of 37%, plastic limit of 23%, and a C_V of 0.331 mm^2/s in a normally consolidated state at a vertical effective stress of 5 to 10 kPa. Based on Ladd and DeGroot (2003), the C_V for a highly OC clay can be estimated to be 5-10 times that of an NC clay, therefore a value of around 3.31 mm^2/s is taken for the kaolin clay.

The penetration velocity was chosen for the penetration tests to be as close as possible to undrained conditions. According to DeJong and Randolph (2012), the drainage conditions during penetration can be determined using the normalized velocity, determined as $V = vD/C_V$. A V greater than 30 is typically indicative

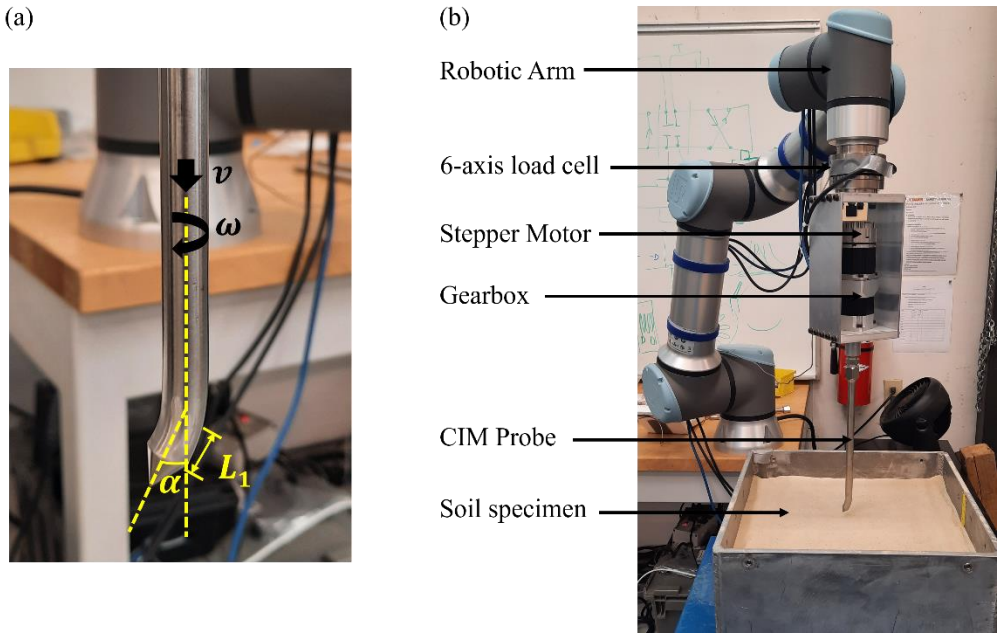

Figure 2. (a) Circumnutation-inspired motion (CIM) probe fabricated for experimental investigation (b) Experimental setup of CIM tests.

of undrained conditions. It should be noted that this framework was developed for CPT penetration, while no solution is available for CIM penetration. For the purposes of this investigation, the vertical velocity of the probe was used in the calculation of V, which is likely to produce an underestimation since the net velocity of any portion of the probe is greater than v due to the rotational action of the probe. Applying this framework indicates that v must be greater than 7.8 mm for undrained conditions. However, the range of required $\omega R/v$ ratios and the maximum ω that the motor and gearbox assembly can apply posed limitations on the maximum v that could be used. A v of 5 mm/s was thus chosen, leading to a V of 19, likely leading to conditions that are close to undrained. The $\omega R/v$ used in the tests were of 0, 0.125, 0.25, 0.5, 1, and 1.57 π.

Initial CPT soundings and CIM tests with low $\omega R/v$ (<0.8 π) showed that the vertical penetration force exceeded the robotic arm's force limit of 150 N (i.e., equivalent to a CPT tip resistance (q_c) of 1.2 MPa), resulting in refusal. Therefore, the initial stage of all the tests involved penetration with an ω = 28.6 RPM ($\omega R/v \approx 0.8\,\pi$) and 42.9 RPM for CIM and CPT tests, respectively, to a depth of 4 cm. After a brief pause, penetration was continued with the target ω for each corresponding test.

2.3. Sand Deposit

The tests on sand were performed in 2 different deposits prepared to the same target conditions. Dry, uniform density sand models were prepared through air pluviation from a fixed drop height to obtain a target relative density of 40%. A poorly graded, sub-angular quartz sand, referred to as "100A" in (Ahmed, Martinez, and DeJong 2023) was used for all tests. The sand has a median particle size of 0.18 mm, 10th percentile particle size of 0.12 mm, coefficient of uniformity of 1.74, coefficient of curvature of 1.04, and critical state friction angle determined from triaxial tests of 32.1°.

The tests were performed in sands at a v of 0.5 mm/s. With this setup, $\omega R/v$ ratios below 0.25 π were not feasible as the resultant ω was too small to be steadily controlled by the motor assembly. Thus $\omega R/v$ ratios of 0, 0.25, 0.5, 1 and 2 π were used for the tests in sand.

3. Results and Discussion

CIM tests with relative velocities ranging from 0 to 2 π were performed in the soil deposits during which the vertical forces and torques were recorded. In addition, CPT tests were performed in each model. Cumulative vertical, rotational, and total work (W_V, W_R and W_T respectively) were then computed from the mobilized vertical forces and torques. The cumulative W_V and W_R for a specific depth were computed as the product of forces and torques with their respective displacements summed over the considered depth (Eq. 1 and 2), while the cumulative W_T at any particular depth is defined as the sum of W_V and W_R (Eq. 3). This study considers a depth of penetration from 6 to 15 cm due to the presence of the stiff crust in the clay model.

$$W_V = \sum_{d_i}^{d_f} F_Z v \Delta t \quad (1)$$

$$W_R = \sum_{d_i}^{d_f} T_Z \omega \Delta t \quad (2)$$

$$W_T = W_V + W_R \quad (3)$$

where d_f is the final depth, d_i is the initial depth, and Δt is the time difference between subsequent data points.

3.1. CIM penetration in Clay

3.1.1. CIM for penetration through stiff crusts

The presence of the crust allowed evaluating the ability of the CIM strategy to help penetrate stiff layers.

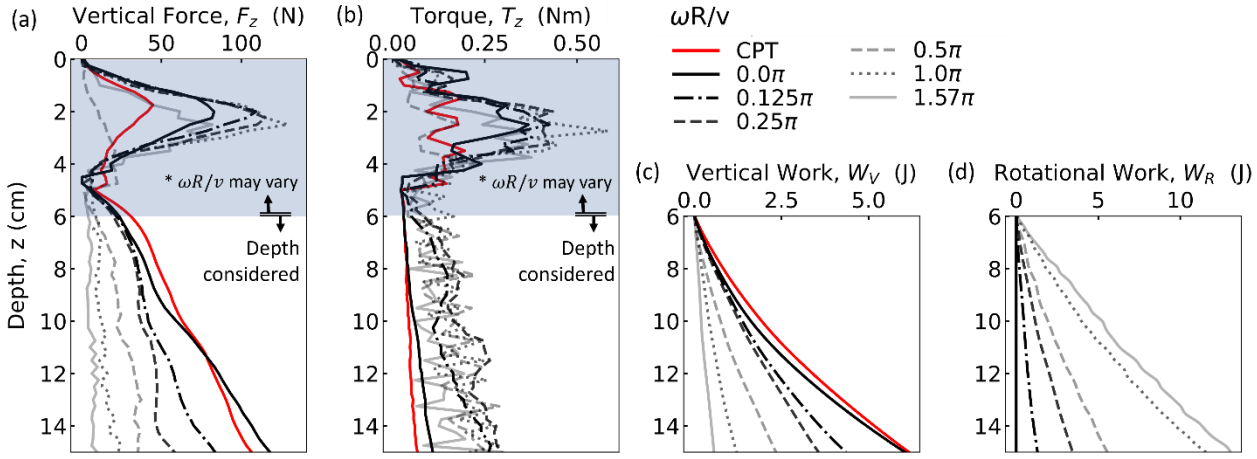

Figure 3. (a) Vertical force and (b) torque mobilized with depth during CIM in clay. *Note the presence of a highly overconsolidated crust at depths smaller than 5 cm, highlighting depth 6-15 cm. An $\omega =$ 28.6 RPM ($\omega R/v \approx 0.8\,\pi$) and $\omega =$ 42.9 RPM used for CIM and CPT probes, respectively, to penetrate the shallow crust indicated by the shading. (c) Vertical work and (d) rotational work done to penetrate the depth considered.

As mentioned in the previous section, CPT and CIM tests with low $\omega R/v$ rations mobilized higher penetration resistance forces than the capacity of the test setup, resulting in refusal. However, as shown in Figure 3a, all the probes successfully penetrated through the stiff layer when ω was large enough (ω= 28.6 RPM, equivalent to $\omega R/v \approx 0.8\,\pi$ for the CIM tests and ω= 42.9 RPM for the CPT test). The forces and torques mobilized in the crust are higher than those in the uniform clay beneath for most $\omega R/v$ values. The peak values in the crust for the CIM tests range between 80 and 125 N; however, the sounding with 0.5 π mobilized a significantly smaller value. This is attributed to spatial variability in the stiff crust. At a depth slightly greater than 4 cm, the F_z and T_z drop to values near zero because the penetration was paused for a few seconds before continuing the sounding with the target $\omega R/v$. Overall, these results validate that introducing an angular velocity reduces the vertical reaction forces required to penetrate stiff layers that could otherwise compromise a sounding.

3.1.2. Force, Torque and Work variation with depth and relative velocity

The vertical forces and torques mobilized during CIM penetration are dependent on the relative velocity, showing consistent trends over different depths. F_z significantly decreases with $\omega R/v$ (Figure 3a), while the CPT mobilizes similar F_z values as the CIM test with an $\omega R/v$ of 0. The T_z values increase with initial increases in $\omega R/v$ but have similar magnitudes with any further increase (Figure 3b). Both the CPT and non-rotating CIM ($\omega R/v$ =0) tests have similar magnitudes of T_z, which are lower than those mobilized during CIM penetration with non-zero $\omega R/v$.

The vertical and rotational works are calculated for depths greater than 6 cm where the influence of the stiff crust is negligible. Both W_V and W_R increase with depth because they represent the cumulative work done to penetrate soil up to a certain depth (Figure 3c and 3d). While W_V exhibits similar reduction with $\omega R/v$ as F_z, W_R increases monotonically with $\omega R/v$ despite T_z reaching stable values due to the linear increase in rotational displacement with $\omega R/v$.

3.2. CIM penetration in Sand

3.2.1. Force, Torque and Work variation with depth and relative velocity

In sand, the variation of F_z and T_z with $\omega R/v$ and depth follow similar trends as in clay, where F_z decreases with increasing $\omega R/v$ (Figure 4a) and T_z increases initially with $\omega R/v$ but plateaus to constant values with further increases (Figure 4b). These trends are also consistent over the range of depth investigated. The F_z and T_z values mobilized during CPT in sand are similar in magnitude to those mobilized during a non-rotational CIM penetration ($\omega R/v$ = 0).

The work components also vary in a similar pattern with $\omega R/v$ and depth as the tests in clay, where W_V decreased while W_R increased with $\omega R/v$ (Figure 4c and 4d). While no crust is present in the sand deposits, the same depths were considered as in the tests in clay for consistency in the comparison presented in the next section.

3.3. Effect of soil type on CIM: clay versus sand

The trends in the variation in F_z, T_z, W_V, and W_R with relative velocity is similar in both clay and sand. Average F_z and T_z values and cumulative W_V and W_R done to penetrate a depth range of 6 to 15 cm are considered to investigate the effect of $\omega R/v$. The magnitude of F_z and T_z mobilized in clay are larger than those mobilized in sand which is expected as the clay is highly overconsolidated and has higher resistance to penetration. In both clay and sand deposits, F_z exponentially decays with $\omega R/v$ while T_z increases from a near zero magnitude for non-rotating CIM and CPT probe to reach stable magnitudes with further increase in $\omega R/v$ (Figure 5a and 5b). While CPT and non-rotating CIM tests are expected to yield a $T_z \approx 0$, a non-zero magnitude of T_z is mobilized likely due to a small offset between the probes' tip and its axis of rotation that were

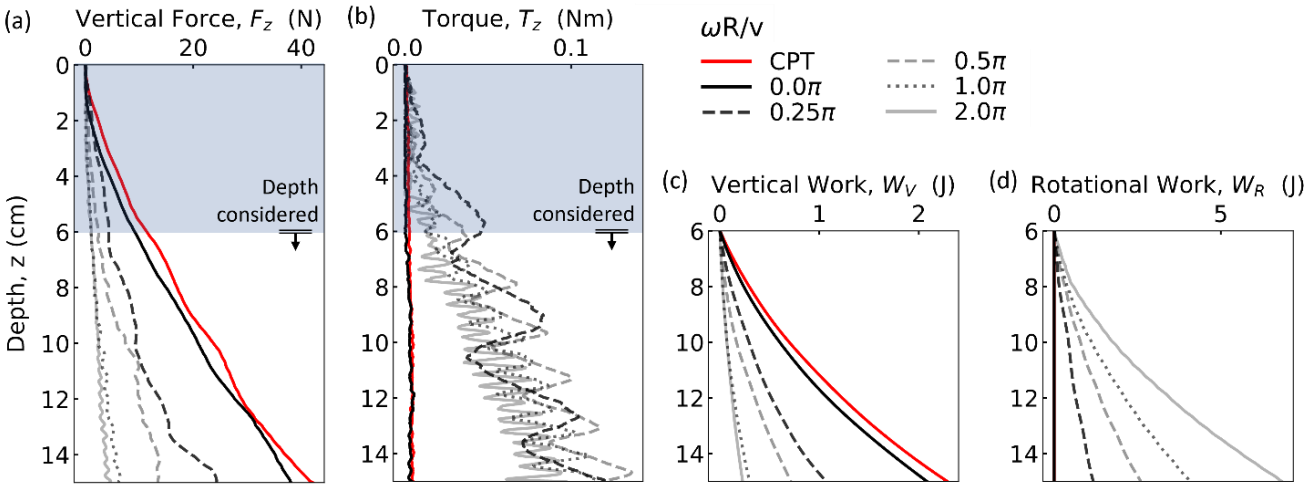

Figure 4. (a) Vertical force and (b) torque mobilized with depth during CIM in sands, highlighting depth 6-15 cm. (c) Vertical work and (d) rotational work done to penetrate the depth considered.

amplified during CIM penetration in the stiff clay. The W_V exponentially decays in a similar fashion as F_z (Figure 5d), while W_R steadily increases with $\omega R/v$ due to the concomitant increase in rotational displacement (Figure 5c and 5e). The total work maintains near-constant magnitudes with initial increases in $\omega R/v$, indicating a similar rate of decrease in W_V as the rate of increase in W_R for low ratios of $\omega R/v$. The rate of decrease in W_V decreases with $\omega R/v$ while the rate of increase in W_R is near-constant with variation in $\omega R/v$. Therefore, the work values increase steadily at $\omega R/v$ values greater than about 0.3 π.

The exponential decays in F_z with $\omega R/v$ for the clay and sand can be represented with an exponential function as shown in Eq. (4):

$$F_z = A\ e^{-B\,(\omega R/v)} + C \tag{4}$$

where the sum of coefficients A and C represent F_z mobilized by a non-rotating CIM probe, the coefficient B represents the rate of decay, and C represents F_z mobilized at larger $\omega R/v$.

The rate of decay is smaller in clay than in sand, with coefficient B values of 2.28 and 2.91, respectively. While the F_z values at high $\omega R/v$ (>1 π) show no significant decrease with further increase in $\omega R/v$ for sand, they continue to decrease, albeit at a low rate, in the clay. For both clay and sand, the F_z at large $\omega R/v$ is reduced by a factor of around 10 in comparison to the non-rotating CIM and CPT tests. This factor of reduction can be quantified by the ratio of the sum of coefficients A and C to the coefficient C (i.e., $(A + C)/C$), which is 9.3 in sand and 11 in clay.

The exponential decay in F_z with $\omega R/v$ is attributed to the rotation of the net direction of soil strain at the probe tip from vertical when ω and $\omega R/v$ are zero towards the horizontal direction as ω and $\omega R/v$ increase. This in turn rotates the resultant direction of the forces mobilized at the probe tip during penetration. While this can successfully explain the trend in F_Z, it would predict a continued increase in T_Z with $\omega R/v$, which contradicts the near-constant or even decreasing trend of the experimental results (Figure 5b). This suggests that the state of stresses around the probe changes with $\omega R/v$, limiting the increase in T_Z. In both clay and sand, the near-constant magnitude that T_z attains with increase in $\omega R/v$ may also be governed by the extent of soil disturbance around the probe. Namely, larger $\omega R/v$ and lower helical trajectory pitch lead to greater amounts of soil strain, and at sufficiently large $\omega R/v$ values the soil around the probe may have reached critical state and offers the same amount of resistance.

Other studies that introduced an angular velocity to CPT probes also found a decrease in vertical resistances and attributed this to change in direction of the resultant forces acting on the probe (Bengough, Mullins, and Wilson 1997; Tang and Tao 2022). The increase in rate of decay of F_z in sand in comparison to clay indicate that this decay is not entirely dependent on the probe geometry and rotation of direction of strain but is also affected by the soil type.

Similar ratios of vertical to torsional resistance is mobilized in clay and sand though this ratio is slightly higher for clay. This is quantified using a non-dimensional parameter $R_{v/h} = F_{v,max}/F_{h,max}$ where $F_{v,max}$ is the maximum F_z obtained for CIM probe and $F_{h,max}$ is the equivalent horizontal resistive force that acts at the tip of the probe (determined using a moment arm of R, i.e., $F_{h,max}$ = $T_{Z,max}$/R) to provide the peak T_z obtained (from Figure 5a and 5b). The $R_{v/h}$ is 1.4 for clay and 1.3 for sand which indicates that the ratio of vertical to torsional resistance during CIM penetration may not be dependent on soil type.

The variation of W_T with $\omega R/v$ is governed by the variation of W_V and W_R, where the influence of W_V decreases with an increase in $\omega R/v$ while the influence of W_R steadily increases. The initial stagnation of the magnitude of W_T with small increases in $\omega R/v$ is due to the opposing trends of W_V's decrease and W_R's increase with $\omega R/v$. Thus, a low relative velocity, $\omega R/v \in (0 - 0.3)$ could be used for CIM penetration without significantly impacting the energy consumption. A dashed line indicating a 25% increase in total work in comparison to a non-rotating CIM test is shown in Figure 5f to indicate a reference $\omega R/v$ at which W_T has not significantly increased. In both clay and sand, the $\omega R/v$

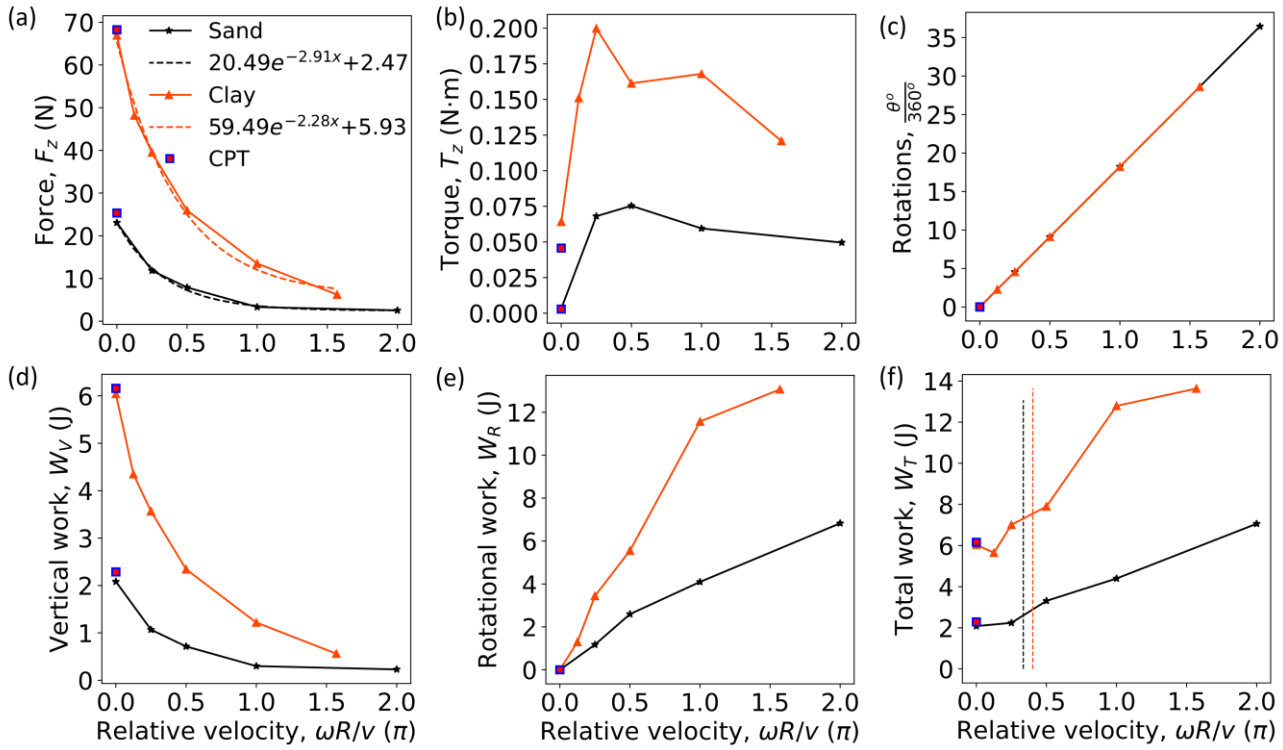

Figure 5. (a) Vertical force and (b) torque (c) rotational displacement (d) vertical work (e) rotational work (f) total work variation with relative velocity for sand and clay.

corresponding to this 25% increase is between 0.25 and 0.5 π. At these $\omega R/v$ ratios, F_z decays by almost half of the F_z of a non-rotating CIM probes in both materials.

Lowering vertical reaction forces needed to penetrate soil while maintaining similar energy consumption compared to conventionally used methods of penetration could allow for use of smaller, light-weight equipment that has an overall lower carbon footprint. Specifically, these rigs would have a similar energy consumption for penetration but a lower fuel consumption for mobilization. For an $\omega R/v$ of 0.3 π, the energy consumption for CIM probes in sand and clay would be around 1.07 and 1.17 of a CPT respectively, while the reaction forces required to penetrate would be 44% and 54% of a CPT respectively. Thus, CIM penetration rigs could potentially be about half the weight of CPT rigs while using only 5-20% more energy for penetration.

4. Conclusions

This study investigates a plant-inspired strategy known as circumnutation-inspired motion to increase the ease and efficiency of soil penetration by virtue of reducing the mobilized vertical resistance while requiring similar amounts of energy. The feasibility of CIM penetration in different soils, a stiff highly over consolidated clay (OCR = 70) and a loose sand (D_R = 40%) are studied by performing experimental tests with CIM probes. The effects of soil type on CIM penetration are studied through the variation of mobilized F_z and T_z and work done as a function of the relative velocity of the probe tip ($\omega R/v$). The test parameters, ω and v were controlled using a robotic arm and a stepper motor and gearbox assembly. CPTs are also performed with probes of the same diameter, apex angle and at the same vertical velocity as the CIM probe in both these soil models for comparison.

This study showcases the use of CIM to penetrate stiff surficial layers when insufficient reaction force can be provided. Specifically, stiff crust in the clay deposit was successfully penetrated with the CIM and CPT probes when an angular velocity was applied to the probe, while penetration attempts without angular velocity were terminated due to refusal.

CIM penetration mobilizes lower vertical resistance but higher torques in comparison to CPTs in both clay and sand. In both soils, the mobilized F_z decayed exponentially with increasing $\omega R/v$ while the T_z increased with initial increases in $\omega R/v$ and reached a near-constant magnitude with further increases. The magnitudes of F_z and T_z mobilized in the stiff clay are higher than those mobilized in the loose sand but vary in a similar fashion with increasing $\omega R/v$. The ratio of maximum vertical to torsional resistance mobilized in both soils are also similar. However, the rate of exponential decay of F_z in the sand is greater than the clay, indicating that this decay is not purely dependent on the motion and geometry of the CIM probe but also on the soil type, which governs the response of the soil around the probe. The W_V and W_R computed from F_z and T_z, respectively, vary in similar fashions with $\omega R/v$ in the clay and sand. Specifically, W_V decays exponentially with $\omega R/v$ (like the variation of F_z with $\omega R/v$) and W_R increases monotonically with $\omega R/v$.

CIM penetration in both soils led to a range of $\omega R/v$ ratios for which the total work the soil does not significantly increase but the mobilized F_z is significantly lower in comparison to non-rotating CIM or CPT penetration ($\omega R/v$ =0). For example, for a 25% increase in W_T, the mobilized F_z reduces by 52% for clay and 55%

for sand compared to the CIM soundings without rotations in the corresponding soils. At a low $\omega R/v$ ratio of 0.3 π, the total energy consumption for penetration (W_T) in both clay and sand increases by less than 20% in comparison to CPT penetration while the reaction forces necessary to penetrate these soils are lower by around 50%.

The findings of this paper suggest that CIM penetration has the potential to significantly reduce the vertical resistances mobilized in different soil types while limiting the amount of energy consumed for penetration. This can be advantageous in minimizing power or energy consumption, and consequently, costs associated with achieving a specific depth in subsurface exploration applications, such as in-situ testing or sensor installation. The significant reduction in vertical resistance observed during CIM penetration could also provide the possibility of utilizing smaller, lightweight penetration equipment, which would lower mobilization costs, increase the accessibility of rigs to congested sites, and reduce the carbon footprint of SI activities. Further investigation on the effect of soil types, depth and confining stress on the forces and torques mobilized during CIM penetration is necessary to facilitate future advancements in this area.

Acknowledgements

The authors express their gratitude to undergraduate students - Fabian Zamora, Junhan Li, and Breiner Rodas, for their help in the preparation of the sand deposit. Special thanks go to Lin Huang, a PhD candidate at the Granular Materials Lab, UC Davis, for generously permitting the use of the clay deposit prepared by him, for centrifuge modelling of offshore anchors, in our experimental investigations on overconsolidated clay. Additionally, the authors extend their appreciation to the faculty and staff at the Centre of Geotechnical Modelling (CGM), UC Davis, for their invaluable support, which played a crucial role in making the experimental setup feasible.

This material is based upon work supported in part by the Engineering Research Center Program of the National Science Foundation under NSF Cooperative Agreement No. EEC–1449501. The authors were supported by the National Science Foundation (NSF) under Award No. 1942369. The preparation of the clay model was conducted at the CGM, UC Davis which is supported under Grant No. CMMI-1520581. Any opinions, findings, and conclusions or recommendations expressed in this material are those of the author(s) and do not necessarily reflect those of the National Science Foundation.

References

Ahmed, Sheikh Sharif, Alejandro Martinez, and Jason T. DeJong. 2023. “Effect of Gradation on the Strength and Stress-Dilation Behavior of Coarse-Grained Soils in Drained and Undrained Triaxial Compression.” *Journal of Geotechnical and Geoenvironmental Engineering* 149 (5): 04023019. https://doi.org/10.1061/JGGEFK.GTENG-10972.

Anilkumar, Riya, Yuyan Chen, and Alejandro Martinez. 2024. “Plant Root-Inspired Soil Penetration in Sands Using Circumnutations for Geotechnical Site Characterization.” In *Geo-Congress 2024*. Vancouver, BC.

Bengough, A. G., C. E. Mullins, and G. Wilson. 1997. “Estimating Soil Frictional Resistance to Metal Probes and Its Relevance to the Penetration of Soil by Roots.” *European Journal of Soil Science* 48 (4): 603–12. https://doi.org/10.1111/j.1365-2389.1997.tb00560.x.

Burrall, Matthew, Jason T. DeJong, Alejandro Martinez, and Daniel W. Wilson. 2020. “Vertical Pullout Tests of Orchard Trees for Bio-Inspired Engineering of Anchorage and Foundation Systems.” *Bioinspiration & Biomimetics* 16 (1): 016009. https://doi.org/10.1088/1748-3190/abb414.

Chen, Yuyan, Ali Khosravi, Alejandro Martinez, and Jason DeJong. 2021. “Modeling the Self-Penetration Process of a Bio-Inspired Probe in Granular Soils.” *Bioinspiration & Biomimetics* 16 (4): 046012. https://doi.org/10.1088/1748-3190/abf46e.

Chen, Yuyan, and Alejandro Martinez. 2023. “DEM Modelling of Root Circumnutation-Inspired Penetration in Shallow Granular Materials.” *Géotechnique*, September, 1–18. https://doi.org/10.1680/jgeot.22.00258.

Darwin, Charles, and Sir Francis Darwin. 1880. *The Power of Movement in Plants*. John Murray.

Davidson, Donald T. 1965. “Penetrometer Measurements.” In *Methods of Soil Analysis*, 472–84. John Wiley & Sons, Ltd. https://doi.org/10.2134/agronmonogr9.1.c37.

DeJong, Jason T., and Mark Randolph. 2012. “Influence of Partial Consolidation during Cone Penetration on Estimated Soil Behavior Type and Pore Pressure Dissipation Measurements.” *Journal of Geotechnical and Geoenvironmental Engineering* 138 (7): 777–88. https://doi.org/10.1061/(ASCE)GT.1943-5606.0000646.

Del Dottore, Emanuela, Alessio Mondini, Ali Sadeghi, Virgilio Mattoli, and Barbara Mazzolai. 2017. “An Efficient Soil Penetration Strategy for Explorative Robots Inspired by Plant Root Circumnutation Movements.” *Bioinspiration & Biomimetics* 13 (1): 015003. https://doi.org/10.1088/1748-3190/aa9998.

Dorgan, Kelly M. 2015. “The Biomechanics of Burrowing and Boring.” *Journal of Experimental Biology* 218 (2): 176–83. https://doi.org/10.1242/jeb.086983.

Huang, Sichuan, and Junliang Tao. 2020. “Modeling Clam-Inspired Burrowing in Dry Sand Using Cavity Expansion Theory and DEM.” *Acta Geotechnica* 15 (8): 2305–26. https://doi.org/10.1007/s11440-020-00918-8.

Martinez, Alejandro, Jason Dejong, Idil Akin, Ali Aleali, Chloe Arson, Jared Atkinson, Paola Bandini, et al. 2022. “Bio-Inspired Geotechnical Engineering: Principles, Current Work, Opportunities and Challenges.” *Géotechnique* 72 (8): 687–705. https://doi.org/10.1680/jgeot.20.P.170.

Martinez, Alejandro, Sophia Palumbo, and Brian D. Todd. 2019. “Bioinspiration for Anisotropic Load Transfer at Soil–Structure Interfaces.” *Journal of Geotechnical and Geoenvironmental Engineering* 145 (10): 04019074. https://doi.org/10.1061/(ASCE)GT.1943-5606.0002138.

Migliaccio, Fernando, Paola Tassone, and Alessio Fortunati. 2013. “Circumnutation as an Autonomous Root Movement in Plants.” *American Journal of Botany* 100 (1): 4–13. https://doi.org/10.3732/ajb.1200314.

Moraes, Moacir T. de, Vanderlei R. da Silva, Anderson L. Zwirtes, and Reimar Carlesso. 2014. “Use of Penetrometers in Agriculture: A Review.” *Engenharia Agrícola* 34 (February): 179–93. https://doi.org/10.1590/S0100-69162014000100019.

O’Hara, Kyle B., and Alejandro Martinez. 2022. “Load Transfer Directionality of Snakeskin-Inspired Piles during Installation and Pullout in Sands.” *Journal of Geotechnical and Geoenvironmental Engineering* 148 (12):

04022110. https://doi.org/10.1061/(ASCE)GT.1943-5606.0002929.

Purdy, Christopher M., Alena J. Raymond, Jason T. DeJong, Alissa Kendall, Christopher Krage, and Jamie Sharp. 2022. “Life-Cycle Sustainability Assessment of Geotechnical Site Investigation.” *Canadian Geotechnical Journal* 59 (6): 863–77. https://doi.org/10.1139/cgj-2020-0523.

Raymond, Alena J., James R. Tipton, Alissa Kendall, and Jason T. DeJong. 2020. “Review of Impact Categories and Environmental Indicators for Life Cycle Assessment of Geotechnical Systems.” *Journal of Industrial Ecology* 24 (3): 485–99. https://doi.org/10.1111/jiec.12946.

Tang, Yong, and Junliang Tao. 2022. “Multiscale Analysis of Rotational Penetration in Shallow Dry Sand and Implications for Self-Burrowing Robot Design.” *Acta Geotechnica*, March. https://doi.org/10.1007/s11440-022-01492-x.

Taylor, Isaiah, Kevin Lehner, Erin McCaskey, Niba Nirmal, Yasemin Ozkan-Aydin, Mason Murray-Cooper, Rashmi Jain, et al. 2021. “Mechanism and Function of Root Circumnutation.” *Proceedings of the National Academy of Sciences of the United States of America* 118 (8): e2018940118. https://doi.org/10.1073/pnas.2018940118.